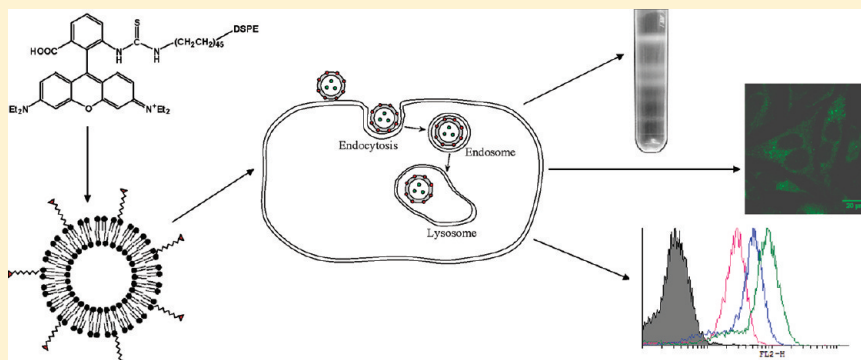


Screening and Optimization of Ligand Conjugates for Lysosomal Targeting

Igor Meerovich, Alexander Koshkaryev, Ritesh Thekkedath, and Vladimir P. Torchilin*

Center for Pharmaceutical Biotechnology & Nanomedicine, Northeastern University, 312 Mugar Hall, 360 Huntington Avenue, Boston, Massachusetts 02115, United States

ABSTRACT:



The use of lysosome-targeted liposomes may significantly improve the delivery of therapeutic enzymes and chaperones into lysosomes for the treatment of lysosomal storage disorders. The aim of this research was to synthesize new potentially lysosomotropic ligands on a base of Neutral Red and rhodamine B and to study their ability to enhance specific lysosomal delivery of surface-modified liposomes loaded with a model compound, fluorescein isothiocyanate-dextran (FD). The delivery of these liposomes and their content to lysosomes in HeLa cells was investigated by confocal immunofluorescent microscopy, subcellular fractionation, and flow cytometry. Confocal microscopy demonstrated that liposomes modified with derivatives of rhodamine B provide a good rate of colocalization with the specific lysosomal markers. The comparison of fluorescence of FD in lysosomes isolated by subcellular fractionation also showed that the efficiency of lysosomal delivery of the liposomal load by liposomes modified with some of synthesized ligands was significantly higher compared to that with plain liposomes. These results were additionally confirmed by flow cytometry of the intact cells treated with liposomes loaded with 5-dodecanoylamino fluorescein di- β -D-galactopyranoside, a specific substrate for the intralysosomal β -galactosidase, using a number of cell lines, including macrophages with induced phenotype of lysosomal enzyme deficiency; two of the synthesized ligands—rhodamine B DSPE-PEG_{2k}-amide and 6-(3-(DSPE-PEG_{2k})-thioureido) rhodamine B—demonstrated enhanced lysosomal delivery, in some cases, higher than that for commercially available rhodamine B octadecyl ester, with the best results (the enhancement of the lysosomal delivery up to 75% greater in comparison to plain liposomes) shown for the cells with induced lysosomal enzyme deficiency phenotype. Use of liposomes modified with rhodamine B derivatives may be advantageous for the development of drug delivery systems for the treatment of lysosome-associated disorders.

INTRODUCTION

Many pharmaceutical agents, including various large (enzymes, antibodies, other polypeptides) and small molecules, must be delivered specifically to particular cell organelles in order to efficiently exert their therapeutic action. Such delivery is still mainly an unresolved problem,¹ although some attempts have been made to target mitochondria and nuclei using liposomes modified with mitochondriotropic² or nucleotropic agents.³

Lysosomes represent one of the important intracellular targets. In a number of inherited human metabolic disorders, the lysosomal storage disorders (LSDs), defects in the lysosomal enzymes, lead to a progressive accumulation of unmetabolized substrates.⁴ LSD symptoms may vary widely depending on the particular mutations inherited and the specific metabolic pathways affected;

LSD clinical manifestations typically include deterioration of neurological function (50% of LSDs are associated with central nervous system (CNS) disorders), as well as pulmonary, hepatic, splenic, cardiovascular, and renal dysfunction. Other tissues and functions also often affected in LSDs include the immune system, bone, connective tissue, skeletal and cardiac muscle, dermis, and ocular function.^{5,6} The clinical course and the severity of individual LSDs usually correlate with levels of residual enzyme activity.

The most extensively used strategy for treatment of LSDs is enzyme replacement therapy (ERT), based on the exogenous

Received: June 27, 2011

Revised: August 24, 2011

Published: September 13, 2011

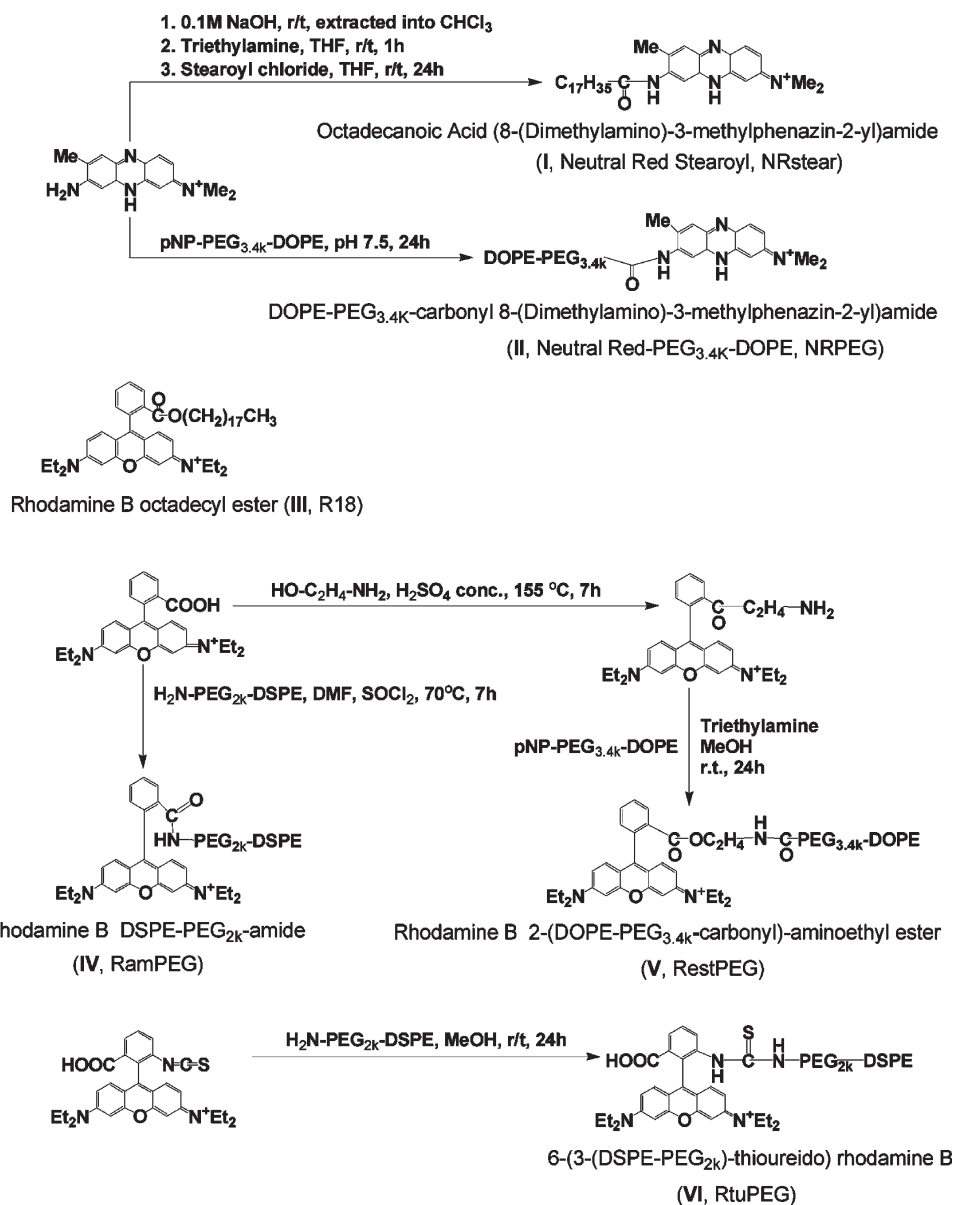


Figure 1. Synthesis of derivatives of Neutral Red and rhodamine B.

administration of active enzymes.⁷ Also, among the potential advances in LSD treatment is the so-called “chaperone therapy”, also called “enzyme enhancement therapy”, aimed at the improperly folded mutant proteins, that are stabilized by the exogenously administered small molecules, resulting in an increase in the levels of functional enzyme. It was shown to be a promising treatment strategy for several LSDs including Gaucher disease, the GM1 and GM2 gangliosidoses, and Fabry disease.⁸ However, this procedure remains limited and expensive because of the instability, poor delivery, and rapid degradation of the administered enzymes.

The use of liposome-immobilized enzymes introduced more than 30 years ago new opportunities for enzyme therapy, especially in the treatment of diseases localized to liver cells which are natural targets for liposomes.⁹ Still, these liposome-based preparations are not in general clinical use for ERT, and a clear need to sharply increase the efficiency of the delivery of the liposomal enzymes to lysosomes inside cells still exists.

Improvement in liposome-based enzyme delivery can be achieved by using liposomes specifically targeted to lysosomes.

Another important aspect related to the lysosomal targeting for drug delivery is the involvement of lysosomes in the treatment of cancer via the activation of the lysosome-dependent cell death pathway.¹⁰ It has been proven that the moderate permeabilization of lysosomal membranes can result in cell apoptosis. On the other hand, secreted lysosomal cathepsins degrade protein components of the extracellular matrix and thus contribute actively to tumor angiogenesis.¹¹ Thus, it may be useful to develop a delivery system with specific lysosomal targeting that can provide inhibition of lysosomal enzymatic activity in cancer cells or deliver lysosome-destabilizing agents that will cause cancer cell apoptosis.

A large variety of small molecules have been identified which specifically target and accumulate in lysosomes. Among them, Neutral Red and rhodamine B are routinely used for the visualization of lysosomes and other acidic organelles in live

cells.^{12,13} The commercially available rhodamine B octadecyl ester is used widely to monitor membrane fusion¹⁴ and for the study of lysosomal metabolism.¹⁵ As shown by Vult von Steyern et al.,¹⁶ rhodamine B accumulates specifically in the lysosomes of denervated skeletal muscle. Huth et al. have shown a preferential build-up of the liposomes within lysosomes, when the liposomal membrane was labeled with rhodamine B-phosphoethanolamine.¹⁷ With this in mind, we originally proved the general concept of the possibility to prepare the lysosome-targeted liposomes based on the use of commercially available Rhodamine B octadecyl ester.¹⁸

The aim of the current work was to synthesize different ligands based on Neutral Red (NR) and rhodamine B (RhB) with short and long poly(ethylene glycol) spacers suitable for introduction into the lipid bilayer and compare their ability to enhance the lysosomal delivery of these ligand-modified liposomes loaded with the model compound FITC-dextran.

MATERIALS AND METHODS

Materials. Egg phosphatidylcholine (ePC), cholesterol (Chol), 1,2-distearoyl-*sn*-glycero-3-phosphoethanolamine-*N*-[amino(polyethylene glycol)-2000] (DSPE-PEG_{2k}-amine) and 1,2-dioleoyl-*sn*-glycero-3-phosphoethanolamine (DOPE) were purchased from Avanti Polar Lipids (Alabaster AL, USA). Fluorescein isothiocyanate-dextran (FD) with molecular weight (MW) of 4400, Neutral Red (NR), rhodamine B (RhB), rhodamine B octadecyl ester (R18), rhodamine B isothiocyanate (RhB-ITC), polyoxyethylene(MW 3400)-bis(*p*-nitrophenyl carbonate) (PEG_{3,4k}-(pNP)₂), triethylamine (TEA), β -galactosidase (product number G0413), protease inhibitor cocktail (PIC), phorbol myristate acetate (PMA), and conduritol B epoxide (CBE) were purchased from Sigma-Aldrich (St. Louis MO, USA). *p*-Nitrophenylcarbonyl-(polyethylene glycol-3400)-dioleoylphosphatidylethanolamine (pNP-PEG_{3,4k}-DOPE) was prepared and purified according to the method in ref 19. Bio-Gel A-1.5 m sorbent was purchased from Bio-Rad (Hercules CA, USA). Lysosome Enrichment Kit, Coomassie-based protein assay kit, and DyLight 350-conjugated goat antimouse IgG were obtained from Pierce Biotechnology (Rockford IL, USA). Fluorescein di- β -D-galactopyranoside (FDG), dodecanoylamino fluorescein di- β -D-galactopyranoside (C₁₂FDG), and 5-(pentafluorobenzoylamino) fluorescein di- β -D-glucopyranoside (PFB-FDGlu) were purchased from Invitrogen/Molecular Probes, Inc. (Eugene OR, USA). Mouse monoclonal (H4B4) anti-lysosome-associated membrane protein antibody (anti-Lamp2) was purchased from Abcam (Cambridge MA, USA). Fluoromount-G mounting medium was purchased from SouthernBiotech (Birmingham AL, USA). Cell cultures of human epithelial cervical cancer CCL-2 (HeLa), mouse melanoma CRL-6475 (B16(F10)), mouse Lewis lung carcinoma CRL-1642 (LLC), mouse embryo fibroblasts CRL-1658 (NIH/3T3), rat myocardium myoblasts CRL-1446 (H9c2), and human monocytes (U-937²⁰) were purchased from the American Type Culture Collection (ATCC, Manassas VA, USA). Cell culture media and supplements were from CellGro (Kansas City MO, USA). All other chemicals and buffer components were analytical-grade preparations. Distilled and deionized water was used in all experiments.

Conjugates of Neutral Red and Rhodamine B. The studied conjugates and paths of their synthesis are shown in Figure 1. Substances were synthesized from commercially available Neutral Red, rhodamine B, and rhodamine B isothiocyanate, except

for rhodamine B octadecyl ester (R18, as ligand **III**), which also was commercially available.

Synthetic Procedures. *Synthesis of Octadecanoic Acid (8-(Dimethylamino)-3-methylphenazin-2-yl)amide (I, NRstear).* **I** was made starting with the Neutral Red acid–base indicator (NR), according to procedure developed by Suzuki et al.²¹ Neutral Red (120 mg) was dissolved in distilled water, and 0.1 M aqueous NaOH was added. The desalted Neutral Red was extracted with chloroform. The organic fraction was dried over Na₂SO₄ and evaporated, resulting in 68.6 mg of free-base form of Neutral Red. The intermediate product and 75 mg of triethylamine (TEA, 7.4 mmol) were dissolved together in 22.5 mL of tetrahydrofuran (THF) and the mixture was stirred for 1 h at room temperature. Stearoyl chloride (128 mg, 0.42 μ mol) of was dissolved with 0.75 mL of THF and added to the reaction mixture, which was stirred for 24 h at room temperature. The THF was evaporated and the residue obtained was dissolved in 20 mL of chloroform. The chloroform phase was washed twice with 20 mL of 1 N HCl and 1 N NaOH, and once with the same deionized water, dried over Na₂SO₄, and evaporated. The residue was purified by silica gel column chromatography with *n*-hexane–ethyl acetate (1:3, *R*_f = 0.83) as the eluent to yield the final product (18.4 mg of purified product, yield 13%). ¹H NMR (CDCl₃, 400 MHz) δ 0.83–0.91 (m, 3H, –CH₃), 1.22–1.43 (m, 30H, –CH₂–), 1.53–1.61 (m, 2H, –CH₂CH₂CO–), 1.75–1.84 (m, 3H, Ar–CH₃), 2.17 (s, 1H, Ar–NH–Ar), 3.19 (s, 6H, Ar=N⁺(CH₃)₂), 3.96–4.00 (m, 1H, Ar–H), 4.19–4.24 (t, *J* = 6.05 Hz), 4.64 (s, 1H, Ar–H), 4.72 (s, 1H, Ar–H), 5.04 (s, 1H, Ar–H), 7.06 (d, *J* = 7.06 Hz, 1H, Ar–H), 7.39 (s, 1H, Ar–H), 7.53 (dd, *J* = 9.64 Hz, 1H, Ar–H), 7.70, 7.90 (s, 1H, Ar–H), 7.98 (d, *J* = 9.61 Hz, 1H, Ar–H).

Synthesis of DOPE-PEG_{3,4k}-carbonyl 8-(Dimethylamino)-3-methylphenazin-2-yl)amide (II, NRPEG). **II** was made from NR by reaction with *p*-nitrophenylcarbonyl-(polyethylene glycol-3400)-dioleoylphosphatidylethanolamine (pNP-PEG_{3,4k}-DOPE), according to ref 19 using less basic conditions (pH 7.5) to avoid precipitation of NR that occurs at pH above 8.0. pNP-PEG_{3,4k}-DOPE (6 mg, 1.37 μ mol) of was dissolved in 2 mL of phosphate buffered saline with pH adjusted to 7.5 containing a 3-fold excess of NR (1.2 mg; 4.15 μ mol). After fully dissolving the pNP-PEG_{3,4k}-DOPE, the resultant mixture was sparged with nitrogen and stirred for 24 h at room temperature. The excess of NR was separated by dialysis against deionized water using Spectra/Por cellulose ester dialysis membranes (Spectrum Laboratories, Rancho Domingues, CA, USA) with a molecular weight cutoff size of 2000 Da. Product was purified from the nonconjugated DOPE-PEG_{3,4k}-COOH by silica gel column chromatography with chloroform–methanol (4:1, *R*_f = 0.65) as the eluent to yield the final product (yield of purified product 2.3 mg, 38%). ¹H NMR (CDCl₃, 400 MHz): δ 0.87–0.89 (m, 6H, –CH₃ of fatty acid chains), 1.00–1.50 (m, 44H, –CH₂– of fatty acid chains), 1.5–1.8 (s, 4H, –COO–CH₂–CH₂–), 1.90–2.14 (m, 8H, –CH₂–CH₂–CH=), 2.20–2.50 (m, 4H, CH₂–CH₂–COO– of fatty acid chains), 3.18 (s, 6H, Ar=N⁺(CH₃)₂), 3.20–3.50 (m, 2H, –CH₂–CH₂–NH₂CO), 3.53–3.78 (m, PEG chains), 3.78–3.85 (m, 2H, CH₂–CH₂–O–), 4.20–4.48 (m, 2H, –O–CH₂–CH(CH₂–/O–), 5.07–5.18 (m, 1H, –O–CH(CH₂–)₂), 5.19–5.41 (m, 4H, –CH=CH–), 6.90–8.00 (m, 5H, Ar–H), 8.06–8.32 (m, 1H, Ar–NH–CO).

Synthesis of Rhodamine B DSPE-PEG_{2k}-amide (IV, RamPEG). **IV** was made from rhodamine B by amidification with

DSPE-PEG_{2k}-amide. Rhodamine B (7.7 mg, 16.1 μ mol) was dissolved in 2 mL of dimethylformamide (DMF). Thionylchloride (2.0 mg, 16.2 μ mol; used as catalyst) was added to the rhodamine B and the mixture was stirred at 55 °C for 40 min. DSPE-PEG_{2k}-amine (15 mg, 5.37 μ mol) was added dropwise to the stirred solution of activated rhodamine B, and the resulting mixture was stirred for additional 7 h at 70 °C under a reverse condenser. The resulting mixture was diluted with deionized water 1:5, and the nonreacted rhodamine B was separated by dialysis against deionized water using Spectra/Por cellulose ester dialysis membranes with cutoff size of 2000 Da. Product was purified from the nonconjugated DSPE-PEG_{2k}-amine by silica gel column chromatography with chloroform–methanol (4:1, R_f = 0.62) as the eluent to yield the final product (yield of purified product 2.0 mg, 11%). ¹H NMR (CDCl₃, 400 MHz): δ 0.87–0.89 (t, 6H, –CH₃ of fatty acid chains), 1.15–1.70 (m, 60H, –CH₂– of fatty acid chains, + 6H, Ar–N(CH₂CH₃)₂), 2.22–2.44 (q, 4H, CH₂–CH₂–COO– of fatty acid chains), 3.18–3.42 (m, 2H, OPO₃–CH₂–CH₂–NH₂CO–Ar=N⁺(CH₃)₂), 3.20–3.50 (m, 2H, –CH₂–CH₂–NH₂CO–), 3.43–4.50 (m, –CH₂–CH₂–O– of PEG chains), 5.07–5.18 (m, 1H, –O–CH(CH₂–)₂), 6.78 (m, 2H, Ar–H), 7.00 (m, 2H, Ar–CONH₂–CH₂), 7.53 (td, 1H, Ar–H), 8.02 (m, 1H, Ar–H).

Synthesis of Rhodamine B 2-(DOPE-PEG_{3,4k}-carbonyl)-aminoethyl Ester (V, RestPEG). V was synthesized starting with the rhodamine B 2-aminoethyl ester, synthesized from rhodamine B as described by Derkacheva et al.²² and generously provided by the authors. Rhodamine B 2-aminoethyl ester (2.6 mg, 4.6 μ mol) was dissolved in 0.5 mL of methanol and activated by adding 0.47 mg (4.6 μ mol) of TEA. pNP-PEG_{3,4k}-DOPE (6 mg, 1.37 μ mol) was dissolved in an activated rhodamine B 2-aminoethyl ester solution. The resultant mixture was sparged with nitrogen and stirred for 24 h at room temperature. The excess of rhodamine B 2-aminoethyl ester was separated by dialysis against deionized water using Spectra/Por cellulose ester dialysis membranes with a cutoff size of 2000 Da. Product was purified from the nonconjugated DOPE-PEG_{3,4k}-COOH by silica gel column chromatography with chloroform–methanol (4:1, R_f = 0.52) as the eluent to yield the final product (yield of purified product 4.0 mg, 62%). ¹H NMR (CDCl₃, 400 MHz) δ 0.84–0.91 (m, 6H, –CH₃ of fatty acids), 1.09–1.20 (m, 6H, Ar–N(CH₂CH₃)₂), 1.23–1.37 (m, 32H, –CH₂– of fatty acids), 1.40–1.43 (m, 6H, Ar=N⁺(CH₂CH₃)₂), 1.54–1.62, 1.66–1.84 (m, 4H, –CH₂–CH₂–COO–), 1.97–2.04 (m, 8H, –CH₂–CH=CH–), 2.24–2.31 (m, 6H, –CH₂–CO–), 3.30–3.38 (m, 2H, –CH₂–NH–COO–), 3.44–3.48 (m, 4H, Ar–N(CH₂–CH₃)₂), 3.54 (s, 2H, –CH₂–NH–CO–), 3.58–3.84 (m, PEG chains), 3.92–4.00, 4.10–4.17 (m, 4H, –PO₄–CH₂–), 4.18–4.22 (m, 2H, –CH₂–O–CO–), 4.36–4.42 (m, 4H, –O–CH(CH₂–O–)₂), 5.18–5.23 (m, 2H, Ar–H and –O–CH(CH₂–O–)₂), 5.29–5.38 (m, 4H, –CH=CH– of fatty acids), 5.84–5.90 (s, 1H, Ar–H), 6.80–6.93 (m, 1H, Ar–H), 7.04–7.20 (m, 2H, Ar–H), 7.27–7.34 (m, 1H, Ar–H), 8.33 (dd, J = 27.89 Hz, 1H, Ar–H).

Synthesis of 6-(3-(DSPE-PEG_{2k})-thioureido) Rhodamine B (VI, RtuPEG). VI was made starting with a rhodamine B isothiocyanate (mix of isomers, from Sigma). Rhodamine B isothiocyanate (7.7 mg, 16.1 μ mol) was dissolved in 1 mL of methanol, and the solution was used to dissolve 15 mg (5.38 μ mol) of DSPE-PEG_{2k}-amine; the resultant mixture was sparged with nitrogen and stirred for 48 h at room temperature. After the reaction, the excess of Rhodamine B isothiocyanate was separated by dialysis against deionized water using Spectra/Por

cellulose ester dialysis membranes with a cutoff size of 2000 Da. Product was purified from the nonconjugated DSPE-PEG_{2k}-amine by silica gel column chromatography with chloroform–methanol (4:1, R_f = 0.56) as the eluent to yield the final product (yield of purified product 5.8 mg, 33%). ¹H NMR (CDCl₃, 400 MHz): δ 0.77–0.99 (m, 6H, –CH₃ of fatty acids), 1.03–1.51 (m, 6H, Ar–N(CH₂CH₃)₂), 1.57–1.72 (m, 4H, –CH₂COO– of fatty acids), 2.01, 2.28–2.39 (m, 4H, –CH₂COO– of fatty acids), 3.21–3.35 (m, 2H, –CH₂–CH₂–NHCOO–) 3.41–3.45 (m, 4H, Ar–N(CH₂CH₃)₂), 3.50–4.25 (m, PEG chains), 5.00–5.18 (m, 1H, Ar–H), 6.23–6.26 (dd, J = 6.26 Hz, 1H, Ar–H), 6.60, 6.80–6.94 (m, 1H, Ar–H), 7.26 (m, 1H, Ar–H), 7.51–7.56 (s, 1H, –CH₂–NH–CS–NH–), 7.69–7.74 (m, 1H, Ar–H), 7.81–7.87 (d, J = 7.83 Hz, 1H, Ar–H).

Preparation of Liposomal Formulations. Plain and ligand-modified FD-loaded liposomes were obtained from lipid films prepared by evaporating the solvent from mixtures of chloroform solutions of egg phosphatidylcholine (ePC) and cholesterol (7:3 molar ratio) in chloroform,¹⁹ optionally supplemented with respective ligands (1 mol %) in ethanol or chloroform. After removing the solvent on a rotary evaporator followed by freeze-drying on a Freeze-Dry System Freezone 4.5 (Labconco, Kansas City, MO), films were redissolved in chloroform and re-dried. The films were hydrated by vigorous vortexing with phosphate-buffered saline (PBS: 137 mM NaCl, 8 mM Na₂HPO₄, 2.7 mM KCl, 1.5 mM KH₂PO₄, pH 7.4) or PBS supplemented with FD (molecular weight 4400, 45 mg/mL) to produce a total lipid content of 10 mg/mL. The hydrated lipid films were extruded 21 times through Nuclepore polycarbonate membranes with 200 nm pore size (Whatman, Clifton, NJ) using an Avanti Mini-Extruder device (Avanti Polar Lipids, Alabaster, AL). Liposomes were separated from non-incorporated FD by gel-filtration on a BioGel 1.5 M column (0.7 \times 24 cm). Final lipid content in the liposomal fraction was calculated from the ratio of volumes of loaded formulation and the eluted fraction. Effective inclusion of FD into liposomes was evaluated using the BioTek Synergy HT microplate reader (BioTek, Winooski, VT) by measuring fluorescence (ex/em: 485/528 nm) of liposomes diluted 1/100 with PBS (pH 7.4) supplied with 0.2% Triton X-100 (to avoid a possible FRET effect), and calculating FD concentration according to a preliminary calibration made under the same conditions, with subsequent normalization to total lipid content.

Alternatively, for the evaluation of lysosomal uptake of the liposomal load by flow cytometry, both plain and ligand-modified liposomes were produced with a load of C₁₂FDG, a 12-carbon lipophilic variant of fluorescein di- β -D-galactopyranoside (FDG).²³ C₁₂FDG solubilized in DMSO was added to a mixture of ePC, Chol, and ligand dissolved in chloroform, at 1.5% molar to total lipids. After evaporation of the solvents, the lipid film was redissolved in chloroform. After a second chloroform evaporation and freeze-drying of the film, C₁₂FDG-loaded liposomes were prepared by hydration of the lipid film in PBS with subsequent extrusion and separation from non-incorporated ligands and C₁₂FDG as described above. To estimate C₁₂FDG loading, C₁₂FDG-liposomes were resuspended in PBS at 150 μ g/mL and incubated with or without recombinant β -galactosidase (0.635 μ g/mL) for 24 h at 37 °C. After the liposome dissolution with 0.2% Triton X-100 (to avoid a possible FRET effect), the fluorescent intensity of the C₁₂-fluorescein produced by enzymatic hydrolysis of C₁₂FDG was measured on a BioTek Synergy HT microplate reader (ex/em: 485/528 nm) and normalized for lipid content.

Characterization of Liposomes. Liposome size distribution was determined by dynamic light scattering using a Coulter N4MD Submicrometer Particle Size Analyzer (Beckman-Coulter, Fullerton, CA). Zeta-potential of liposomal preparations was measured at 25 °C in 0.1 mM KCl solution (diluted to a lipid content of 0.2–0.3 $\mu\text{g}/\text{mL}$) using the Zeta-Plus Instrument (Brookhaven Instruments, Holtsville, NY).

Cell Cultures. The fluorescent microscopy and subcellular fractionation studies were done on HeLa cells, used for experiments up to passage 16. For the cell experiments, HeLa cells were grown at 37 °C at 5% CO_2 and 95% humidity in Dulbecco Modified Eagle's medium (DMEM) supplemented with 10% fetal bovine serum (FBS), 100 U/mL penicillin, 100 $\mu\text{g}/\text{mL}$ streptomycin, and 2 mM glutamine. To reseed the cell cultures or harvest them for subcellular fractionation or flow cytometry studies, cells were detached by trypsinization with 0.5% trypsin in PBS containing 0.025% EDTA. B16(F10), LLC, NIH/3T3, and H9c2 cells were grown and treated according to the same general protocol.

The U-937 monocytes, that were used for modeling the phenotype of lysosomal enzyme deficiency disorder, were grown in flasks suspended in RPMI-1640 medium supplemented with 10% FBS, 100 U/mL penicillin, 100 $\mu\text{g}/\text{mL}$ streptomycin, and 2 mM glutamine. To induce the needed phenotype, the cells were first seeded in 6-well plates 5×10^6 cells per well in complete RPMI-1640 and cultured for 48 h in the presence of 10nM phorbol myristate acetate (PMA; Sigma-Aldrich).²⁴ The mature attached macrophages were washed twice with the sterile PBS and cultured for an additional 72 h in complete RPMI-1640, supplied with 200 μM of conduritol B epoxide (CBE; Sigma-Aldrich).^{25,26} To harvest the macrophages for flow cytometry studies after the incubation with liposomes, the cells were detached using 4 mg/mL lidocaine in PBS containing 0.025% EDTA.

Lysosomal β -Glucocerebrosidase Enzymatic Activity Assay. The efficiency and stability of the induction of the lysosomal enzyme deficiency phenotype in U-937 cells were evaluated by the residual enzymatic activity of the lysosomal β -glucocerebrosidase after the treatment of the cells with PMA and CBE immediately, as well as after different recovery times after the removal of the CBE-containing medium replaced by the fresh complete RPMI-1640 medium. For this evaluation, the cells were seeded and subsequently treated with PMA and CBE as described above. At specific time points after removal of the CBE, the cells were detached using lidocaine and EDTA, dispersed in 300 μL of PBS (pH 7.4), supplemented with 50 μM of specific β -glucocerebrosidase substrate, 5-(pentafluorobenzoylamino) fluorescein di- β -D-glucopyranoside (PFB-FDGlu), and incubated for 1 h at 37 °C. Residual enzymatic activity, resulting in the formation of the fluorescent fluorescein derivative, was evaluated from the intensity of the green fluorescence determined at the emission wavelength of 520 nm (channel FL-1) by flow cytometry, with macrophages not treated with the CBE as a control.

Interaction of Liposomes with Cells *in Vitro*. Cells grown to the needed extent of confluence were incubated with liposomes added at amounts calculated to provide the same FD or C_{12}FDG load to cells for every liposomal formulation, in their respective serum-free media for 4 h, then washed twice with medium to remove nonbound liposomes and used for studies. When required, cells treated with liposomes for 4 h were washed twice with fresh medium to remove nonbound liposomes and incubated for an additional chase period of 20 h at 37 °C in 5% CO_2 in

complete liposome-free medium (denoted further in the text as 4 + 20 h incubation).

Immunofluorescence Microscopy. Intracellular trafficking and localization of FD-loaded ligand-modified liposomes were preliminarily tested using a fluorescent microscope Nikon Eclipse E400 (Japan) equipped with a 6 V-20W halogen lamp, filter blocks for blue (EX/DM/BA 330–380/400/435 nm), green (465–495/505/515–565), and red (528–553/565/600–600) spectral channels and 100 \times oil-immersion objective. After the initial evaluation, the samples obtained by incubation of cells with liposomes that provided better colocalization with lysosomes were re-evaluated using a Zeiss LSM 700 upright confocal microscope (Thornwood, NY) equipped with a 63 \times , 1.4-numerical aperture plan-apochromat oil-immersion objective. HeLa cells were grown on microscope coverslips in 6-well plates seeded in complete DMEM medium at 10^4 cells per well. When cells reached 40–50% confluence, plain and ligand-modified liposomes were added to cells in amounts providing an equal FD load for all formulations with an average concentration of total lipids 50 $\mu\text{g}/\text{mL}$ and incubated as described. After incubation, cells were washed with PBS and fixed with 4% paraformaldehyde in PBS (pH 7.4) for 15 min at room temperature (RT), followed by a PBS wash, quenching with NaBH_4 in PBS for 5 min, and another PBS wash. The cells were then permeabilized by incubation with 0.2% saponin and 1% BSA in PBS for 10 min at RT, washed three times with a blocking solution (1% BSA in PBS, pH 7.4), and kept for 30 min in the same buffer. The cells were stained with the mouse antihuman Lamp2 mAb diluted with blocking solution (1:50) for 60 min at RT, and washed five times with the blocking solution. Visualization was achieved by cell incubation with DyLight 350-conjugated goat antimouse IgG (1:100 dilution) for 60 min at RT followed with five washes with the blocking solution. Individual coverslips were mounted cell-side down onto fresh glass slides with fluorescence-free glycerol-based mounting medium (Fluoromount-G; Southern Biotechnology Associates, Inc.) and studied under bright light and under epifluorescence with UV, Rhodamine/TRITC, and Fluorescein/FITC filters. Co-localization of liposomes and lysosomal markers was characterized for individual cells ($N = 8$ to 20 for different liposomal formulations) by Pearson's correlation coefficient (PCC) and Manders' overlap coefficient (MOC),²⁷ calculated using *ImageJ* 1.42 software (National Institutes of Health, Bethesda, MD) with MBF bundle of plug-ins (McMaster University, Hamilton, ON, Canada).

Evaluation of Lysosomal Delivery by Subcellular Fractionation. HeLa cells were grown to 90% confluence under the above-described conditions and incubated with liposomes added at amounts calculated to provide the same FD load on cells for all formulations in complete DMEM for 4 + 20 h.

In order to isolate the lysosome-enriched fractions, the cells (~ 0.7 – 1.0×10^8 cells per sample) were collected by trypsinization and washed with ice-cold PBS. The cell pellet was resuspended in 1 mL of the reagent A of the Lysosome Enrichment Kit (Pierce Biotechnology, Rockford IL, USA) complemented with 1% (v/v) of a protease inhibitor cocktail. After 2 min incubation on ice, the cells were lysed by sonication (20 bursts, 3 s each, at 6 W). The cell lysate was treated with 1 mL of the reagent B of the same kit. The mixture was gently shaken several times and centrifuged at 500 g for 10 min at 4 °C to pellet nuclei and any remaining intact cells. The postnuclear supernatant was then adjusted with OptiPrep gradient medium

Table 1. Composition and Properties of Plain and Ligand-Modified Liposomal Formulations

liposomal formulation	composition (mol %)				size \pm SD (nm)	zeta \pm SD (mV)	FD/lipids (mg/mg)	C ₁₂ FDG loading (% to Lip-C ₁₂ FDG)
	ePC	Chol	ligand	C ₁₂ FDG				
Lip-FD	70	30	—	—	200 \pm 70	-13.7 \pm 6.5	0.31 \pm 0.16	—
Lip-C12FDG	70	30	—	1.5	205 \pm 85	-10.1 \pm 1.2	—	100
Lip-NRstear-FD	70	30	1	—	210 \pm 72	-8.1 \pm 4.9	0.06 \pm 0.01	—
Lip-NRPEG-FD	70	30	1	—	169 \pm 47	-20.1 \pm 4.6	0.17 \pm 0.01	—
Lip-RestPEG-FD	70	30	1	—	153 \pm 27	-31.0 \pm 8.2	0.25 \pm 0.02	—
Lip-R18	70	30	1	—	232 \pm 51	11.5 \pm 2.5	—	—
Lip-R18-FD	70	30	1	—	240 \pm 75	-6.4 \pm 4.6	0.28 \pm 0.15	—
Lip-R18-C12FDG	70	30	1	1.5	201 \pm 40	-10.2 \pm 1.0	—	112 \pm 30
Lip-RamPEG	70	30	1	—	208 \pm 30	-0.6 \pm 3.1	—	—
Lip-RamPEG-FD	70	30	1	—	179 \pm 68	-5.2 \pm 0.5	0.39 \pm 0.12	—
Lip-RamPEG-C12FDG	70	30	1	1.5	180 \pm 49	-33.3 \pm 4.4	—	145 \pm 37
Lip-RtuPEG	70	30	1	—	198 \pm 42	-0.3 \pm 1.3	—	—
Lip-RtuPEG-FD	70	30	1	—	179 \pm 44	-11.4 \pm 7.3	0.26 \pm 0.07	—
Lip-RtuPEG-C12FDG	70	30	1	1.5	184 \pm 65	-28.1 \pm 3.5	—	119 \pm 29

(Pierce Biotechnology; 60% v/v solution of Iodixanol) to 15% of Iodixanol, loaded onto the top of discontinuous density gradient with the following steps from top to bottom: 17%, 20%, 23%, 27%, and 30% of Iodixanol (by respective dilutions of OptiPrep), and subjected to ultracentrifugation at 145 000 g for 2 h at 4 °C using Beckman Coulter Optima XL ultracentrifuge equipped with SW41Ti swinging bucket rotor (Beckman Coulter, Krefeld, Germany). A total of 5 resultant fractions were collected from the top of the tube, diluted with PBS to the equal total volume of 6 mL, pelleted at 30 000 g for 30 min at 4 °C using Beckman Coulter Optima TLX Tabletop equipped with TLA-100.3 fixed angle rotor (Beckman Coulter, Krefeld, Germany), and then resuspended in equal volumes of cold PBS. All collected fractions were evaluated for lysosomal β -galactosidase activity and analyzed for protein, FD, and ligand content.

Protein concentration in each fraction was determined using a Coomassie protein assay in triplicate by measuring absorption at 595 nm using BioTek Synergy HT microplate reader (BioTek Instruments, Winooski, VT, USA). FD and ligand content in fractions were determined by measuring the fluorescence intensity of equal volumes of each fraction in triplicate, using the same microplate reader at 485/528 nm and 530–590 nm (ex/em), respectively. The quantity of FD in each subcellular fraction was calculated using a calibration by standard FD solutions in PBS.

The lysosomal β -galactosidase activity was evaluated by dispersing 50 μ L of each fraction in 150 μ L of PBS supplemented with 15 μ M of fluorescein di- β -D-galactopyranoside (FDG) and incubating the mix for 18 h at 37 °C. The intensity of fluorescence of the resultant product was measured using a microplate reader at 485/528 nm.

Measured and calculated values for each ligand, FD, and relative β -galactosidase activity were normalized to the protein content, and their fractional distribution was calculated as a percent of the normalized value in each fraction to the total sum of all fractions.

Flow Cytometry Analysis. The binding of plain and rhodamine-based ligand-modified liposomes to cultured cells was evaluated by flow cytometry. Control (untreated) HeLa cells or cells treated with liposomes were washed twice with DMEM

and trypsinized. The harvested cells were washed twice with PBS, resuspended in 1 mL of ice-cold PBS, and their fluorescence determined using a fluorescence-activated cell sorter (FACS). Data acquisition was performed on a Becton Dickinson FACScan (Becton Dickinson, San Jose, CA), and the data were analyzed using *CellQuest* software (Becton Dickinson). The green and red fluorescence were determined respectively at the emission wavelengths of 520 and 580 nm (channels FL-1 and FL-2). To eliminate possible overlap of rhodamine fluorescence with channel FL-1, the compensation between FL-1 and FL-2 channels was applied using the cells incubated with nonloaded ligand-modified liposomes as an additional control.

The data were tested for statistical significance using the Student's paired *t* test. *P*-values were considered significant at *p* \leq 0.05.

RESULTS

All liposomal formulations were characterized for size, zeta-potential, and FD or relative C₁₂FDG content (see Table 1).

In all cellular studies *in vitro*, liposomes were added for incubation with cells at dilutions providing the same FD or C₁₂FDG load to cells for all liposomal formulations.

Intracellular Localization of Ligand-Modified Liposomes. The lysosomotropic ability of ligands was initially tested by fluorescent microscopy of HeLa cells incubated with plain or ligand-modified FD-loaded liposomes, fixed and treated as described in Methods.

Both derivatives of Neutral Red showed low or no colocalization of liposomal FD with antibody-marked lysosomes (PCC/MOC for Lip-NRstear-FD and Lip-NRPEG-FD liposomes were, respectively, -0.032/0.007 and 0.403/0.567) and were excluded from further study, while samples of cells incubated with rhodamine B derivatives showed elevated colocalization of liposomal load in comparison to plain Lip-FD liposomes under the same conditions and were reanalyzed using the more accurate method of confocal microscopy.

Figures 2 and 3 show representative confocal fluorescence micrographs of HeLa cells incubated with plain or ligand-modified

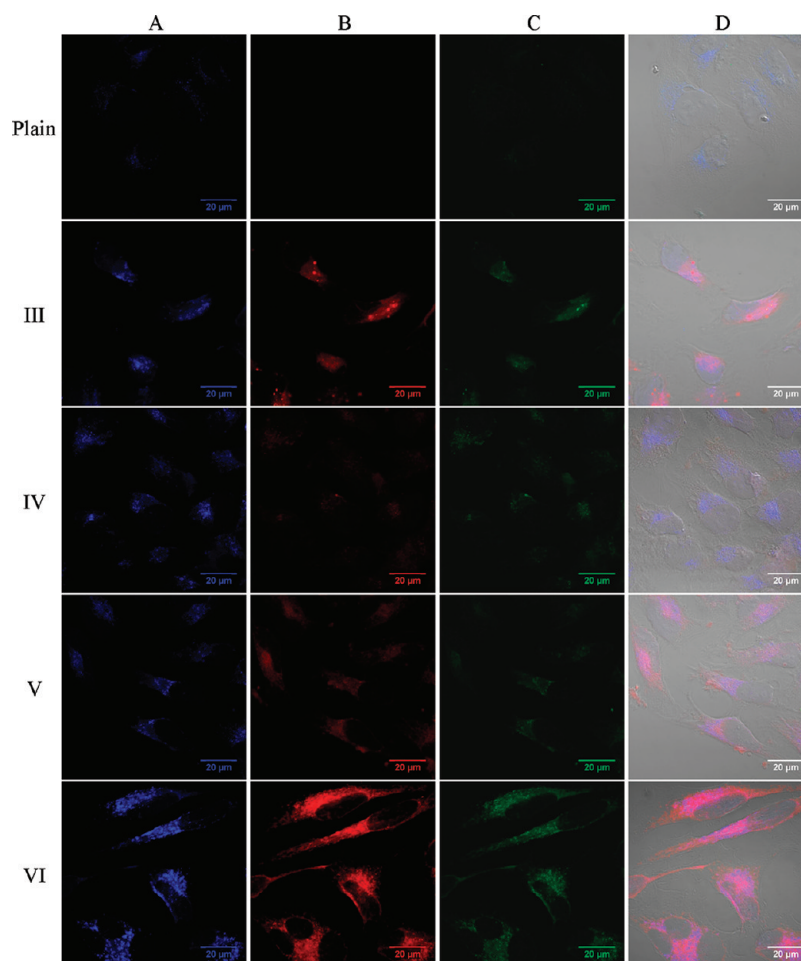


Figure 2. Confocal microscopy images of the intracellular distribution of FD-loaded liposomes modified with rhodamine B derivatives (incubation 4 h). Rows: “Plain” — cells incubated with plain Lip-FD liposomes (as control), rows III to VI — cells incubated, respectively, with Lip-R18-FD, Lip-RamPEG-FD, Lip-RestPEG-FD, and Lip-RtuPEG-FD liposomes. Columns: A (blue channel) — fluorescence of anti-Lamp2 antibody-stained lysosomes; B (red channel) — fluorescence of RhB-derivative modified liposomes; cells incubated with plain liposomes were not observed under this regime, respective position Plain-B is filled with a blank panel; C (green channel) — fluorescence of FITC-dextran; D — Overlay of A, B, and C images with their respective DIC image. Scale bar = 20 μm .

FD-loaded liposomes for 4 h, without and with an additional chase period of 20 h.

Estimation of colocalization of ligand-modified liposomes with lysosome-specific marker (Table 2) after 4 h of incubation showed that liposomes with rhodamine B derivatives provided a much higher rate of lysosomal localization in comparison to such for plain FD-loaded liposomes (MOP = 0.410; PCC = 0.619).

An additional chase period of 20 h after the 4 h incubation of cells with liposomes generally decreased the colocalization of FITC-dextran with anti-Lamp2 mAb-labeled lysosomes for both plain and ligand-modified liposomes. However, lysosomal colocalization of FD delivered by rhodamine-conjugated liposomes remained significantly higher than for plain Lip-FD liposomes (Figure 3, Table 2).

Evaluation of Intracellular Distribution of FD-Loaded Ligand-Modified Liposomes Incubated with Cultured HeLa Cells, by Subcellular Fractionation. To study the organelle distribution of ligand-modified liposomes and their FD load by subcellular fractionation, the cultured HeLa cells were incubated for 4 + 20 h with liposomes diluted to provide the same FD load on cells, originally chosen to keep the average liposomal

lipid load of 50 $\mu\text{g}/\text{mL}$ and then kept at the same level (9.8 $\mu\text{g}/\text{mL}$).

As shown by β -galactosidase activity assay, about 60% of the lysosomal β -galactosidase was concentrated in fraction 1 with a minor part (about 20%) in fraction 2 and negligible amounts in other fractions.

The fractional distribution of each ligand was calculated as a percent of the fluorescence measured at 530/590 nm (ex/em) for each fraction and normalized to the protein content to the total sum of normalized fluorescent intensities of fractions 1 to 5. Results shown in Figure 4A demonstrate that most of all rhodamine B-based liposome-attached ligands accumulated in the lysosome-enriched fractions (about 50% in fraction 1 or 60–70% in fractions 1 + 2).

The fractional distribution of absolute protein-normalized content of FD is demonstrated in Figure 4B. The absolute accumulation of FD in the first fraction compared with the value for the same fraction from fractionation of cells incubated with plain FD-loaded liposomes showed statistical significant difference for Lip-R18-FD ($p = 0.05$) and Lip-RtuPEG-FD ($p = 0.005$), with more moderate enhancement for Lip-RamPEG-FD

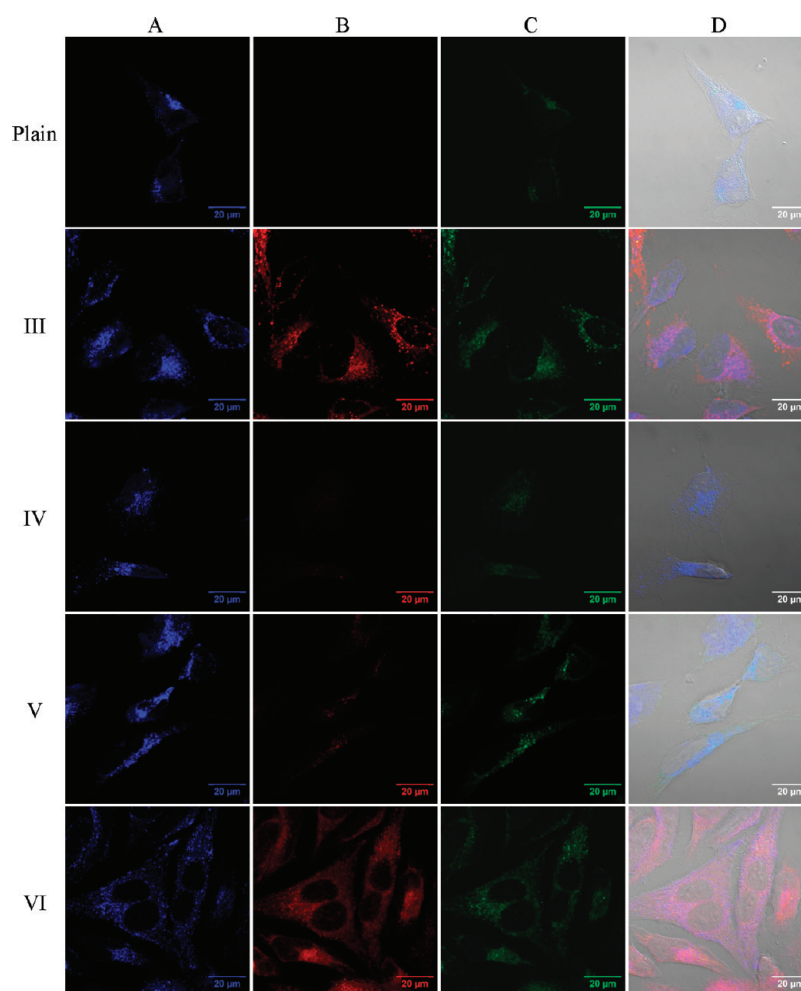


Figure 3. Confocal microscopy images of the intracellular distribution of FD-loaded liposomes modified with rhodamine B derivatives (incubation 4 + 20 h). Rows: “Plain” — cells incubated with plain Lip-FD liposomes (as control); rows III to VI — cells incubated respectively with Lip-R18-FD, Lip-RamPEG-FD, Lip-RestPEG-FD, and Lip-RtuPEG-FD liposomes. Columns: A (blue channel) — fluorescence of anti-Lamp2 antibody-stained lysosomes; B (red channel) — fluorescence of RhB-derivative modified liposomes; cells incubated with plain liposomes were not observed under this regime, respective position Plain-B is filled with blank panel; C (green channel) — fluorescence of FITC-dextran; D — Overlay of A, B, and C images with their respective DIC image. Scale bar = 20 μm .

Table 2. Averaged Coefficients of Colocalization of Ligand-Modified Liposomes and Liposomal FD Load with Anti-Lamp2 mAb Labeled Lysosomes, Determined from Micrographs Obtained by Confocal Immunofluorescent Microscopy^a

liposomal formulation	incubation 4 h				incubation 4 + 20 h			
	Ligand to anti-Lamp2 mAb		FD to anti-Lamp2 mAb		Ligand to anti-Lamp2 mAb		FD to anti-Lamp2 mAb	
	PCC	MOC	PCC	MOC	PCC	MOC	PCC	MOC
Lip-FD (Plain)	—	—	0.410	0.619	—	—	0.363	0.508
Lip-R18-FD (III)	0.769	0.864	0.756 ^{***}	0.857 ^{***}	0.708	0.791	0.726 ^{**}	0.808 ^{**}
Lip-RamPEG-FD (IV)	0.637	0.790	0.656 ^{**}	0.769 ^{**}	0.523	0.693	0.588 [*]	0.735 ^{**}
Lip-RestPEG-FD (V)	0.726	0.816	0.604 ^{**}	0.745 ^{**}	0.544	0.711	0.613 ^{**}	0.760 ^{**}
Lip-RtuPEG-FD (VI)	0.816	0.877	0.862 ^{***}	0.902 ^{***}	0.695	0.805	0.632 ^{**}	0.767 ^{**}

^a PCC — Pearson’s correlation coefficient, MOC — Mander’s overlap coefficient. Values are presented as mean for *N* cells (*N* = 8 to 20 for different liposomal formulations). * *p* < 0.05. ** *p* < 0.01. *** *p* < 0.001.

and absence of FD delivery enhancement for Lip-RestPEG-FD liposomes (Table 3). The observed increase of FD fluorescence was not determined by a possible overlap of RhB and FITC

spectral channels as was shown previously for liposomes modified with rhodamine B octadecyl ester¹⁸ by comparing the green channel fluorescence of fractions obtained from nontreated cells

or cells incubated with ligand-modified liposomes without a FD load.

Thus, liposomes modified with R18, RtuPEG, and RamPEG which demonstrated enhancement of lysosomal delivery of their FD load were chosen for further studies.

Flow Cytometric Evaluation of General Uptake of Ligand-Modified Liposomes by Cell. The general interaction of cells with FD-loaded liposomes modified with rhodamine-based ligands (R18, RtuPEG, and RamPEG) was evaluated with tumor (HeLa and B16(F10)) and normal (NIH/3T3 and H9c2) cell lines using the flow cytometry method.

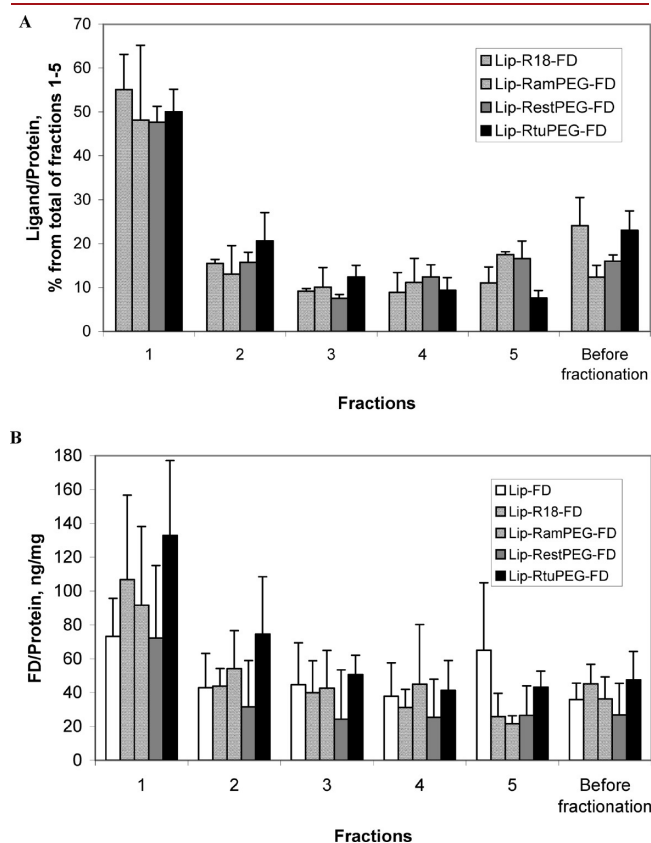


Figure 4. Relative fractional distribution of protein-normalized fluorescence of rhodamine B derivatives (A) and fractional distribution of protein-normalized FD content (B) in fractionated HeLa cells incubated with different ligand-modified liposomes for 4 + 20 h (number of experiments $n = 6$).

Liposomes were added to cells in amounts calculated to provide the same total FD content in cell medium (originally chosen to have average lipid load on cells $100 \mu\text{g}/\text{mL}$, then kept the same) of $36.44 \mu\text{g}/\text{mL}$. After incubation with liposomes for 4 h, cells were harvested as described in Methods and used for measurements. Since used cell lines had different autofluorescence, results were presented as relative FL-1 fluorescence values normalized to the value of FL1 for nontreated cells.

Results are shown in Table 4. In most cases, cells incubated with FD-loaded liposomes surface-modified with rhodamine B derivative ligands showed a significant increase of FL-1 channel fluorescence in comparison to plain FD-loaded liposomes.

Evaluation of Lysosomal Targeting by Flow Cytometry Using Liposomes Loaded with C_{12} FDG. To additionally confirm and compare the ability of liposomes modified with rhodamine B derivatives to specifically target lysosomes, we evaluated their specific lysosomal targeting by flow cytometric analysis of live cells using liposomes loaded with C_{12} FDG, a lipophilic substrate for the lysosomal β -galactosidase, as was proposed in ref 18, assuming FL1 fluorescence will be emitted only by product of its hydrolysis by lysosomal β -galactosidase (C_{12} -fluorescein).

The plain and ligand-modified liposomal formulations were prepared, loaded with C_{12} FDG and characterized as described in Methods. Despite the introduction of C_{12} FDG into the lipid bilayer of the liposomes, its effective load (evaluated by β -galactosidase cleavage of C_{12} FDG localized on the surface of the intact liposomes) varied between plain and ligand-modified liposomes. Because of this, we studied the lysosomal uptake of ligand-modified liposomes with intact cultured cells, adding the liposomal formulations to cells in amounts that provided the same total load of C_{12} FDG as plain C_{12} FDG-loaded liposomes at concentration of $200 \mu\text{g}/\text{mL}$ by total lipids.

The lysosomal uptake was evaluated on a number of cultured tumor and normal cell lines including HeLa, B16(F10) melanoma, LLC carcinoma, NIH/3T3 fibroblasts, and H9c2 myoblasts.

Considering the general purpose of the study, the enhancement of the lysosomal load was also specially evaluated on U-937 monocytes matured to macrophages with induced phenotype of lysosomal enzymatic deficiency disorder.^{24–26} The acquisition of the lysosomal enzyme deficiency phenotype by the cells was confirmed by evaluation of the residual lysosomal β -glucocerebrosidase enzymatic activity (see Methods) immediately as well as 24, 48, and 72 h after the removal of the CBE-containing medium. It was observed that, immediately after the removal of the CBE, the cells retained about 35% of the β -glucocerebrosidase activity of the control (macrophages without CBE treatment).

Table 3. Characterization or Intracellular Distribution of Liposomal FD Delivered by Different Ligand-Modified Liposomes

liposomal formulation	relative content of FD in fraction 1 (% from total sum of fractions 1 to 5)	content of FD in fraction 1 (ng/mg proteins)	content of FD in loaded lysate, (ng/mg proteins)	paired <i>t</i> test of FD content	
				in fraction 1 against the fraction 1 of sample incubated with plain FD-loaded liposomes (<i>P</i> -value)	ratio of FD contents in fraction 1 and loaded nuclei-free lysate
Lip-FD	27.8 ± 8.5	73.2 ± 22.5	35.9 ± 9.7	—	2.04
Lip-R18-FD	43.1 ± 20.2	106.7 ± 50.0	45.2 ± 11.5	0.05	2.36
Lip-RamPEG-FD	35.9 ± 18.3	91.6 ± 46.5	36.3 ± 12.9	0.19	2.52
Lip-RestPEG-FD	40.1 ± 23.8	72.3 ± 42.8	26.8 ± 18.7	0.94	2.70
Lip-RtuPEG-FD	38.7 ± 12.9	132.8 ± 44.3	47.6 ± 16.8	0.005	2.79

Table 4. General FD Delivery to Cells by Ligand-Modified Liposomes

liposomal formulation	cell line			
	HeLa	B16(F10)	NIH/3T3	H9c2
Ratios of Averaged Normalized General Uptake of FD by Different Cells (By Values of Fluorescence Intensity in FL-1 Channel) Provided by Ligand-Modified Liposomes to the Value for Plain Liposomes ^a				
Lip-R18-FD	1.73	1.55	1.25	1.40
Lip-RamPEG-FD	1.65	1.38	0.90	1.24
Lip-RtuPEG-FD	1.67	1.97	1.16	1.43
Paired <i>t</i> test of Averaged Normalized General Uptake of FD Provided by Ligand-Modified Liposomes in Comparison with the Value for Plain Liposomes (<i>P</i> -value)				
Lip-R18-FD	0.0001	0.013	0.036	0.03
Lip-RamPEG-FD	0.0001	0.002	0.237	0.02
Lip-RtuPEG-FD	0.0003	0.002	0.006	0.05

^a Due to different autofluorescence of cell lines, values of FL-1 fluorescence of cells incubated with liposomes were used normalized to the respective values for nontreated cells. Number of experiments *n* = 3 to 6.

Table 5. Lysosomal Uptake of C₁₂FDG Delivered to Cells by Ligand-Modified Liposomes

liposomal formulation	cell line					
	HeLa	B16(F10)	LLC	NIH/3T3	H9c2	U-937
Ratios of Averaged Normalized Lysosomal Uptake of C ₁₂ FDG by Different Cells (By Values of Fluorescence Intensity in FL-1 Channel) Provided by Ligand-Modified Liposomes to the Value for Plain Liposomes ^a						
Lip-R18-C ₁₂ FDG	1.17	1.09	1.47	1.04	1.15	1.35
Lip-RamPEG-C ₁₂ FDG	1.27	1.02	1.15	1.22	1.12	1.75
Lip-RtuPEG-C ₁₂ FDG	1.12	1.26	1.29	1.13	1.16	1.55
Paired <i>t</i> test of Averaged Normalized Lysosomal Uptake of C ₁₂ FDG Provided by Ligand-Modified Liposomes in Comparison with the Value for Plain Liposomes (<i>P</i> -value)						
Lip-R18-C ₁₂ FDG	0.013	0.024	0.00002	0.073	0.014	0.149
Lip-RamPEG-C ₁₂ FDG	0.017	0.38	0.001	0.001	0.020	0.0074
Lip-RtuPEG-C ₁₂ FDG	0.035	0.003	0.021	0.005	0.007	0.0004

^a Due to different autofluorescence of cell lines, values of FL1 fluorescence of cells incubated with liposomes were used normalized to the respective values for nontreated cells. Number of experiments *n* = 3 to 6.

The enzymatic activity recovered to 47–49% of control by 24–48 h post-CBE removal and to 62% after 72 h. All experiments with flow cytometric evaluation of the lysosomal delivery of liposomal load with activated U-937 cells were performed within a short time range after induction of the lysosomal deficiency by adding the liposome-containing medium immediately after removal of CBE.

The results presented in Table 5 show that, for all tested cell lines, the cells incubated with C₁₂FDG-loaded liposomes modified with rhodamine B derivatives used demonstrated significantly increased C₁₂FITC fluorescence compared to the cells treated with the plain liposomes, for at least two out of three ligands. The extent of the enhancement of the lysosomal targeting of the model substance (and the ligand providing the best enhancement) differed among cell lines, achieving the maximum values for cells with the induced phenotype of lysosomal disorder.

DISCUSSION

In our earlier paper,¹⁸ we demonstrated that liposomes modified with rhodamine B octadecyl ester acquire the ability to specifically target lysosomes and allow for an increased

delivery of a liposome-entrapped model substance (FITC-dextran with a relatively high molecular mass of 4400 Da) to these organelles.

In the current study, we attempted to develop and study other potential lysotropic ligands based on commercially available rhodamine B and Neutral Red, routinely used for the visualization of lysosomes in live cells.^{12,13} A number of liposomal formulations with a ligand-modified surface were prepared using synthesized RhB and NR derivatives and loaded with FD. Their interaction with cultured cells and the ability to deliver FD to lysosomes were investigated using fluorescent microscopy, subcellular fractionation, and flow cytometry in comparison to plain FD-loaded liposomes and previously studied liposomes modified with rhodamine B octadecyl ester.

The fluorescent microscopy studies have demonstrated that liposomes modified with RhB derivatives generally show an elevated colocalization of both the liposome-attached ligand and loaded FD with a specific lysosomal marker Lamp2 (visualized using anti-Lamp2 monoclonal antibodies), while liposomes modified with derivatives of NR show much less effect. Additional study by subcellular fractionation of cells incubated with FD-loaded liposomes modified with rhodamine B derivatives and comparison of the fluorescence of lysosome-enriched fractions

with those for the cells treated with control nonmodified liposomes confirmed the lysosome-targeting ability of three rhodamine B derivatives.

Since methods such as cell staining for microscopy or subcellular fractionation of cell lysates are considered disruptive, this tendency was checked on intact live cells of several cell lines by flow cytometry, proving both an increased general accumulation of rhodamine-modified liposomes by cells and their increased delivery into the lysosomes, thus confirming the data obtained by microscopy and subcellular fractionation methods.

The evaluation of the specific lysosomal delivery of a model drug substance by liposomes modified with rhodamine B derivatives showed the best results for the cells with an induced phenotype of a lysosomal enzyme deficiency disorder (the enhancement of the lysosomal uptake of C₁₂FDG by different rhodamine B-based conjugates in the range 35–75% in comparison to nonmodified liposomes). Still, it should be noted that the development of drug delivery systems for specific LSDs, such as Gaucher disease, GM1 and GM2 gangliosidoses, and Fabry disease, requires evaluation of the efficiency of lysosomal delivery by those systems using the respective specific cell lines and animal models.

CONCLUSION

The study has demonstrated that modification of the liposomal surface with Rhodamine B-based ligands increases the delivery of liposomal FITC-dextran to lysosomes. Liposomes modified with two of the synthesized ligands—rhodamine B DSPE-PEG_{2k}-amide and 6-(3-(DSPE-PEG_{2k})-thioureido) rhodamine B—enhance lysosomal delivery of model drug load *in vitro*, in some cases, higher than commercially available rhodamine B octadecyl ester and can be used for further investigation and potentially for development of drug forms for the treatment of the lysosomal storage disorders. The choice of the optimal rhodamine B-based ligand and the extent of the lysosomal delivery enhancement *in vitro* depend on the cell line. Still, the best results (the enhancement of the lysosomal delivery up to 75% greater in comparison to plain liposomes) has been shown for the cells with induced lysosomal enzyme deficiency phenotype.

AUTHOR INFORMATION

Corresponding Author

*Vladimir P. Torchilin, Ph.D., D.Sc., Professor and Director, Center for Pharmaceutical Biotechnology and Nanomedicine, Northeastern University, 312 Mugar Hall, 360 Huntington Ave., Boston, MA 02115. E-mail: v.torchilin@neu.edu. Phone: 617-373-3206. Fax: 617-373-4201.

ACKNOWLEDGMENT

The research was funded by NIH grant RO1 CA 128486 to Vladimir P. Torchilin.

ABBREVIATIONS

ePC, egg phosphatidylcholine; Chol, cholesterol; DSPE-PEG_{2k}-amine, 1,2-distearoyl-*sn*-glycero-3-phosphoethanolamine-*N*-[amino-(polyethylene glycol)-2000]; DOPE, 1,2-dioleoyl-*sn*-glycero-3-phosphoethanolamine; FD, fluorescein isothiocyanate-dextran; NR, Neutral Red; RhB, rhodamine B; R18, rhodamine B octadecyl ester; RhB-ITC, rhodamine B isothiocyanate; PEG_{3,4k}- (pNP)₂, polyoxyethylene(MW 3400)-bis(p-nitrophenyl carbonate);

TEA, triethylamine; PIC, protease inhibitor cocktail; PMA, phorbol myristate acetate; CBE, conduritol B epoxide; pNP-PEG_{3,4k}-DOPE, p-nitrophenylcarbonyl-(polyethylene glycol-3400)-dioleoyl-phosphatidylethanolamine; mAb, monoclonal antibody; IgG, immunoglobulin G; FDG, fluorescein di- β -D-galactopyranoside; C₁₂FDG, dodecanoylamino fluorescein di- β -D-galactopyranoside; PFB-FDGlu, 5-(pentafluorobenzoylamino) fluorescein di- β -D-glucopyranoside; anti-Lamp2, mouse monoclonal (H4B4) antilyosome-associated membrane protein antibody; THF, tetrahydrofuran; NRstear, octadecanoic acid (8-(dimethylamino)-3-methylphenazin-2-yl)amide; NRPEG, DOPE-PEG_{3,4k}-carbonyl 8-(dimethylamino)-3-methylphenazin-2-yl)amide; RamPEG, rhodamine B DSPE-PEG_{2k}-amide; RestPEG, rhodamine B 2-(DOPE-PEG_{3,4k}-carbonyl)-aminoethyl ester; RtuPEG, 6-(3-(DSPE-PEG_{2k})-thioureido) rhodamine B; FBS, fetal bovine serum; PBS, phosphate buffered saline; RT, room temperature; BSA, bovine serum albumin; DIC, differential interference contrast; PCC, Pearson's correlation coefficient; MOC, Mander's overlap coefficient; FACS, fluorescence-activated cell sorter; Lip, liposomes; EDTA, ethylenediaminetetraacetic acid; SD, standard deviation

REFERENCES

- (1) Torchilin, V. P. (2006) Recent approaches to intracellular delivery of drugs and DNA and organelle targeting. *Annu. Rev. Biomed. Eng.* 8, 343–75.
- (2) Boddapati, S. V., D'Souza, G. G., Erdogan, S., Torchilin, V. P., and Weissig, V. (2008) Organelle-targeted nanocarriers: specific delivery of liposomal ceramide to mitochondria enhances its cytotoxicity *in vitro* and *in vivo*. *Nano Lett.* 8, 2559–63.
- (3) Ko, Y. T., Kale, A., Hartner, W. C., Papahadjopoulos-Sternberg, B., and Torchilin, V. P. (2009) Self-assembling micelle-like nanoparticles based on phospholipid-polyethyleneimine conjugates for systemic gene delivery. *J. Controlled Release* 133, 132–8.
- (4) Raas-Rothschild, A., Pankova-Kholmyansky, I., Kacher, Y., and Futerman, A. H. (2004) Glycosphingolipidoses: beyond the enzymatic defect. *Glycoconj. J.* 21, 295–304.
- (5) Scriver, C. R., Sly, W. S., Childs, B., Beaudet, A. L., Valle, D., Kinzler, K. W., and Vogelstein, B. (2000) *The Metabolic and Molecular Bases of Inherited Disease*, 8 ed., McGraw-Hill Professional, New York.
- (6) Muro, S. (2010) New biotechnological and nanomedicine strategies for treatment of lysosomal storage diseases. *Wiley Interdiscip. Rev. Nanomed. Nanobiotechnol.* 2, 189–204.
- (7) Grabowsky, G. A., and Desnick, R. J. (1981) Enzyme replacement in genetic diseases, *Enzymes as Drugs* (Holcenberg, J. S., and Roberts, J., Eds.) Wiley, New York.
- (8) Butters, T. D. (2007) Pharmacotherapeutic strategies using small molecules for the treatment of glycolipid lysosomal storage disorders. *Expert Opin. Pharmacother.* 8, 427–35.
- (9) Gregoriadis, G. (1978) Liposomes in the therapy of lysosomal storage diseases. *Nature* 275, 695–6.
- (10) Kirkegaard, T., and Jaattela, M. (2009) Lysosomal involvement in cell death and cancer. *Biochim. Biophys. Acta* 1793, 746–54.
- (11) Boya, P., Andreau, K., Poncet, D., Zamzami, N., Perfettini, J. L., Metivier, D., Ojcius, D. M., Jäättelä, M., and Kroemer, G. (2003) Lysosomal membrane permeabilization induces cell death in a mitochondrion-dependent fashion. *J. Exp. Med.* 197, 1323–1334.
- (12) Horobin, R. W. (2002) Xanthenes. *Conn's Biological Stains: A Handbook of Dyes, Stains and Fluorochromes for Use in Biology and Medicine* (Horobin, R. W., Kiernan, J. A., and Conn, H. J., Eds.) p 237, Chapter 16, BIOS Scientific Publishers, Oxford, U.K.
- (13) Minier, C., and Moore, M. N. (1996) *Mar. Ecol.: Prog. Ser.* 142, 165–173.
- (14) Hoekstra, D., de Boer, T., Klappe, K., and Wilschut, J. (1984) Fluorescence method for measuring the kinetics of fusion between biological membranes. *Biochemistry* 23, 5675–5681.

(15) Kuwana, T., Mullock, B. M., and Luzio, J. P. (1995) Identification of a lysosomal protein causing lipid transfer, using a fluorescence assay designed to monitor membrane fusion between rat liver endosomes and lysosomes. *Biochem. J.* 308, 937–946.

(16) Vult von Steyern, F., Josefsson, J. O., and Tagerud, S. (1996) Rhodamine B, a fluorescent probe for acidic organelles in denervated skeletal muscle. *J. Histochem. Cytochem.* 44, 267–74.

(17) Huth, U., Wieschollek, A., Garini, Y., Schubert, R., and Peschka-Suss, R. (2004) Fourier transformed spectral bio-imaging for studying the intracellular fate of liposomes. *Cytometry A* 57, 10–21.

(18) Koshkaryev, A., Thekkedath, R., Pagano, C., Meerovich, I., and Torchilin, V. P. (2011) Targeting of lysosomes by liposomes modified with octadecyl-rhodamine B. *J. Drug Targeting*, Epub ahead of print (DOI: 10.3109/1061186X.2010.550921).

(19) Torchilin, V. P., Levchenko, T. S., Lukyanov, A. N., Khaw, B. A., Klibanov, A. L., Rammohan, R., Samokhin, G. P., and Whiteman, K. R. (2001) p-Nitrophenylcarbonyl-PEG-PE-liposomes: fast and simple attachment of specific ligands, including monoclonal antibodies, to distal ends of PEG chains via p-nitrophenylcarbonyl groups. *Biochim. Biophys. Acta* 1511, 397–411.

(20) Sundstrom, C., and Nilsson, K. (1976) Establishment and characterization of a human histiocytic lymphoma cell line (U-937). *Int. J. Cancer* 17, 565–77.

(21) Suzuki, K., Hirayama, E., Sugiyama, T., Yasuda, K., Okabe, H., and Citterio, D. (2002) Ionophore-based lithium ion film optode realizing multiple color variations utilizing digital color analysis. *Anal. Chem.* 74, 5766–5773.

(22) Derkacheva, V. M., Mikhalenko, S. A., Solov'eva, L. I., Alekseeva, V. I., Marinina, L. E., Savina, L. P., Butenin, A. V., and Luk'yanets, E. A. (2007) Phthalocyanines and related compounds: XLIV. Synthesis of conjugates of phthalocyanines with rhodamines. *Russian Journal of General Chemistry* 77, 1117–1125.

(23) Plovins, A., Alvarez, A. M., Ibanez, M., Molina, M., and Nombela, C. (1994) Use of fluorescein-di-beta-D-galactopyranoside (FDG) and C12-FDG as substrates for beta-galactosidase detection by flow cytometry in animal, bacterial, and yeast cells. *Appl. Environ. Microbiol.* 60, 4638–41.

(24) Baek, Y. S., Haas, S., Hackstein, H., Bein, G., Hernandez-Santana, M., Lehrach, H., Sauer, S., and Seitz, H. (2009) Identification of novel transcriptional regulators involved in macrophage differentiation and activation in U937 cells. *BMC Immunol.* 10, 18.

(25) Newburg, D. S., Shea, T. B., Yatziv, S., Raghavan, S. S., and McCluer, R. H. (1988) Macrophages exposed in vitro to conduritol B epoxide resemble Gaucher cells. *Exp. Mol. Pathol.* 48, 317–23.

(26) Yatziv, S., Newburg, D. S., Livni, N., Barfi, G., and Kolodny, E. H. (1988) Gaucher-like changes in human blood-derived macrophages induced by beta-gluco-cerebrosidase inhibition. *J. Lab. Clin. Med.* 111, 416–20.

(27) Manders, E. M. M., Verbeek, F. J., and Aten, J. A. (1993) Measurement of co-localisation of objects in dual-colour confocal images. *J. Microsc.* 169, 375–382.